



# Effect of water on the rock strength and creep behavior of green mudstone

Jinduo Li · Yuan Gao · Tianhong Yang ·  
Penghai Zhang · Wenxue Deng · Feiyue Liu

Received: 5 October 2022 / Accepted: 21 January 2023  
© The Author(s) 2023

**Abstract** The weakening of rock mass after immersion substantially affects slope stability. Considering the mudstone in the north slope of the Fushun West Open pit as the research object, we investigated the failure and creep characteristics of mudstone under different immersion times and confining pressures. For this, we used a self-developed experimental apparatus that applies biaxial compression loading in a water immersion environment. Water significantly changed the strength and failure mode of the mudstone. The increase in confining pressure limits the expansion of the crack aperture, reduces the rock strength-weakening coefficient, and delays the rock weakening time. The change in cohesion is primarily responsible for the weakening of shear strength during immersion. Based on the creep test results, the creep curve of the soaking specimen was identical to that of the dry specimen in the initial phase. The

weakening effect of water on the specimen increased as the soaking duration increased, due to which the creep curve of the soaking specimen gradually approached that of the saturated specimen. Water entered the microcracks and reacted with the rock interior, accelerating rock failure. Consequently, the soaking specimen had the lowest stress level for creep failure and the shortest failure time. The results of this experiment provide a reference for the long-term stability of the flooded slope.

## Highlights

1. Development of experimental equipment, considering the water–rock interaction of bank slope.
2. Increase in confining pressure reduces the weakening effect of water on rock during water soaking.
3. Analysis of creep behavior of dried, saturated, and soaking specimens showed that soaking has the shortest failure time.

---

J. Li · Y. Gao · T. Yang (✉) · P. Zhang (✉) · W. Deng  
Center for Rock Instability and Seismicity Research,  
School of Resources and Civil Engineering,  
Northeastern University, Shenyang 110819, Liaoning,  
People's Republic of China  
e-mail: yangtianhong@mail.neu.edu.cn

P. Zhang  
e-mail: zhangpenghai@mail.neu.edu.cn

F. Liu  
State Key Laboratory of Mining Response and Disaster  
Prevention and Control in Deep Coal Mine, Anhui  
University of Science and Technology, Huainan 232001,  
Liaoning, China

**Keywords** Mudstone · Soaking time · Creep ·  
Experiment study · Failure · Weakening coefficient

## 1 Introduction

The presence of water considerably influences the geotechnical slope stability (Sun et al. 2022; Mikroutsikos et al. 2021). Studies have shown that fluctuating water levels are the main factor causing reservoir bank landslides (Gutierrez et al. 2010; Jiao et al. 2014; Huang 2018). Jones et al. (1961) found that 50% of the landslides were triggered in periods of rising water levels and approximately 30% during the drawdown stage in the Grand Coulee dam reservoir in the United States from 1941 to 1953. Subsequently, Nakamura (1990) reported that approximately 60% of landslides in Japanese reservoirs were triggered during the drawdown operation and 40% were due to water impoundment. Rainfall was reported as another factor responsible for the occurrence of landslides on reservoir slopes (Macfarlane 2009; Chen and Wu 2018; Tu et al. 2019). Therefore, deeply investigating the slope stability under water conditions is important.

The Fushun West Open-pit in China is the largest modern open-pit in Asia, with a length of approximately 6.6 km from east to west, a width of approximately 2.2 km from south to north, and a depth of approximately 420 m (Zhang et al. 2019; Wang et al. 2010; Johnson 1990). In mining, the slope stability and rock mass deformation characteristics of the Fushun Open-pit have been studied by several researchers. Yang et al. (2014) and Yuan et al. (2021) investigated the rheological characteristics of mudstone in the north slope by using a shear creep test, and determined the rheological model to predict the long-term stability of the slope. Zhang et al. (2021) used a microseismic technique, field investigation, and numerical analysis to study the sliding mass depth and deformation control of the Fushun West Open-pit. In addition, researchers have used high-resolution remote sensing and DInSAR to analyze the relationship between the slope deformation and mining activities of Fushun West Open-pit (Liu et al. 2015; He et al. 2015). This open-pit will become an important reservoir in the future. The lithology of the north slope of the open-pit is mainly green mudstone, whose mechanical properties are extremely sensitive to water. Additionally, many important industrial and residential buildings are located near the north slope. Thus, an elaborate investigation of post-closure slope

stability in the process of water immersion before water storage is necessary.

Most failures of the bank slope are due to gradual evolution, which means that before the failure, the slope undergoes continuous deformation. Therefore, evaluating the rock water-weakening effect and quantifying the time-dependent deformation are crucial in bank slope safety assessment. Environmental factors, such as differential stress, confining pressure, temperature and pore fluid composition can strongly influence the creep characteristics of rock (Brantut et al. 2013; Rybacki et al. 2015, 2016; Bonnelye et al. 2017; Li et al. 2019; Tarifard et al. 2022). Among them, water has a greater influence on clay-rich rocks, and the presence of the swelling clay mineral makes them extremely sensitive to water (Geng et al. 2017, 2018; Baud et al. 2000). Mudstone is a typical clay-rich sedimentary whose water sensitivity has attracted much attention from researchers. As documented by Brady and Weil (1960) and Israelachvili and Mcguigan (1988), mudstone contains clay minerals such as montmorillonite; thus, it easily expands and disintegrates after being saturated with water. Dan et al. (2012) suggested that water is an important factor affecting the disintegration of mudstone, and the higher the water content of the mudstone, the higher its disintegration rate. Huang et al. (2007) hypothesized that the real cause of mudstone disintegration in water is linked to characteristics of internal structure, not the content of montmorillonite. Farulla et al. (2010) observed that in addition to the structural characteristics (types and contents) of clay minerals, external environmental factors are an important part of the disintegration characteristics. Rybacki et al. (2017) demonstrated that the long-term creep behavior of clay-rich rock is related to the proportion of high and low strength minerals, and suggested that stress corrosion may aggregate the propagation and closure of microcracks during creep deformation. The mudstone in the bank slope experiences continuous disintegration which can reduce its strength and the slope safety factor, therefore, an intensive study on the strength weakening mechanism of mudstone after immersion in water is of substantial research and engineering significance.

Most researchers first immersed rock specimens in water for a specific period, and then removed and placed them in a testing machine for testing (Tang

2018; Yu et al. 2019). However, most reservoir bank slopes are dry before impoundment. Notably, when the slope is filled with water, the water–rock interaction occurs first on the slope surface and the lateral pressure gradient decreases as the infiltration range deepens. Therefore, the stress state of the slope surface can be simplified as follows: one side is affected by water pressure, and the other five sides are affected by the rock mass confining pressure, as shown in Fig. 1. To improve the research on the long-term stability of the surrounding rock under water immersion, we developed a device to investigate the deterioration mechanism of mudstone in the north slope of Fushun West Open pit based on the perspective of unilateral immersion of the slope. Moreover, we also investigated the failure modes and strength weakening characteristics of mudstone under various confining pressures and immersion times. Additionally, mudstone was immersed in water for creep testing and compared with dried and saturated specimens. Finally, the strain, creep rate, and threshold stress for different water contents were analyzed based on the experimental results. This study provides references for the long-term stability and deformation prediction of bank slopes.

## 2 Methodology

### 2.1 Experimental methods

This study mainly examined the effect of water on the mechanical behavior of rocks under low confining pressure. The intermediate principal stress ( $\sigma_2$ ) values were 0, 0.5, 1, 1.5, and 2 MPa. When the intermediate principal stress ( $\sigma_2$ ) value was  $>0.5$  MPa,

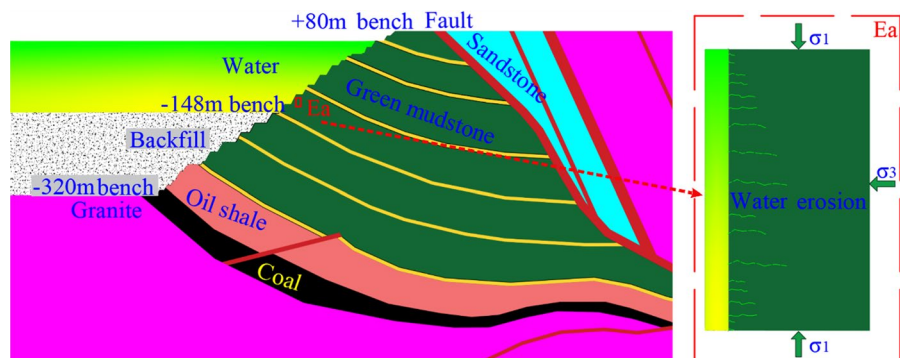
the minimum principal stress ( $\sigma_3$ ) value was set at 0.5 MPa. In the immersion experiment, the application of confining pressure does not contribute to the effective measurement of the water content of the rock specimen. Therefore, the effect of water on rock can only be approximated based on immersion time. In this study, the immersion times were 10, 30, and 60 min.

The uniaxial compressive strength (UCS) of specimens with different water contents were tested at room temperature (25 °C) and 40% humidity to examine the relationship between water content, soaking time, and rock strength. During UCS testing, axial load was increased at a rate of 0.5 MPa/s.

Next, the mechanical behavior of multiple specimen groups was tested under different confining pressures and immersion times. The dried specimens were placed inside a water tank and subjected to axial and confining pressure loading. When the confining pressure became stable and reached a certain value, water was injected into the tank until the rock was completely submerged. After immersion in water for a certain period of time, it was loaded axially until it failed. The purpose of this test was to investigate the effect of water on the mechanical behavior of the rock under different confining pressures and to determine the stress level to be applied in the creep test.

Finally, for the creep test, three groups of green mudstone specimens were prepared: dried, saturated, and soaking specimens. The dried specimens were placed in a humidifier, and their quality was measured every 24 h. When the change in quality of specimens did not exceed 0.1%, the water content was considered to have reached a stable state and the specimen was considered as a saturated specimen. The soaking

**Fig. 1** Cross-section of water–rock interaction during water immersion in Fushun West Open pit



specimen was dry before loading but was immersed in water from the beginning to the end of the creep test. When  $\sigma_2$  was 2 MPa and  $\sigma_3$  was 0.5 MPa, the dried, saturated, and soaking specimens were tested. In the creep test, the creep characteristics of rock can be well reflected via multi-stress level loading (Ma 2004; Xue et al. 2021, 2023). The stress increment at each level was 4 MPa, and the loading time was 10 h.

The water content ( $w_t$ ), softening coefficient ( $\eta_{ct}$ ), and ratio of creep strain ( $\omega$ ) were considered for analyzing experimental results using the following equations:

$$w_t = \frac{m_t - m_d}{m_d} \times 100\% \quad (1)$$

where  $m_d$  denotes the mass of dried specimens and  $m_t$  denotes the mass of the specimens soaked in water for various durations.

$$\eta_{ct} = \frac{\sigma_{cwt}}{\sigma_c} \quad (2)$$

where  $\sigma_c$  denotes the strength of dried specimens and  $\sigma_{cwt}$  denotes the strength of specimens soaked in water for various durations.

$$\omega = \frac{\varepsilon_c}{\varepsilon_0} \times 100\% \quad (3)$$

where  $\varepsilon_c$  denotes the creep strain and  $\varepsilon_0$  denotes the initial strain.

## 2.2 Rock sample preparation

In this study, all specimens were obtained from newly mined green mudstone rock blocks at E2400 of the north slope of Fushun West Open pit (an elevation of  $-200$  m). According to the standards of the International Society for Rock Mechanics (ISRM) (ISRM 2007), rock specimens measuring 100 mm in height and 50 mm in width were cut using a STX-1202A diamond wire cutting machine (Fig. 2). The dry cutting method was used to prevent water from damaging rock samples during cutting. The white bedding shown in Fig. 4 represents the rock sample powder that was not cleaned during sample preparation and does not represent the real bedding of the rock sample. In the Fushun West Open pit, the sampling rate of mudstone is approximately 40%, and the total sample preparation time is approximately 3 months.

The ranges of the mass and wave velocity of specimens without surface cracks were 3,000–3,200 m/s and 576–578 g, respectively. The specimens with deep cracks accounted for 15% of the total rock samples, and their mass and wave velocity were  $<574$  g and 2500 m/s, respectively. The wave velocity, mass, and UCS of the specimens with less developed surface cracks were similar to those of intact rocks. The mudstone specimens with several cracks were removed before drying. The specimens having a mass of 576–578 g and wave velocity of 3000–3200 m/s were selected and then dried in a drying oven at



(a) Rock blocks of green mudstone



(b) Specimens of green mudstone

**Fig. 2** Specimens derived from green mudstone



110 °C for 24 h (ASTM 2005). Only 10% of the dried specimens showed surface crack propagation and surface spalling, and the mass and wave velocity of these rock samples exhibited significant changes. Therefore, we eliminated these specimens. Finally, the remaining selected rock samples were used for testing.

Figure 3 shows that the rock particles are generally green, contain pores, and have no bedding structure; this observation is consistent with those in the literature (Sun et al. 2022). X-ray diffraction analysis revealed that green mudstone mainly comprises 44% muscovite, 19.6% feldspar, 19.6% analcime, and 11.9% montmorillonite, with the remaining content being perovskite. Montmorillonite is a

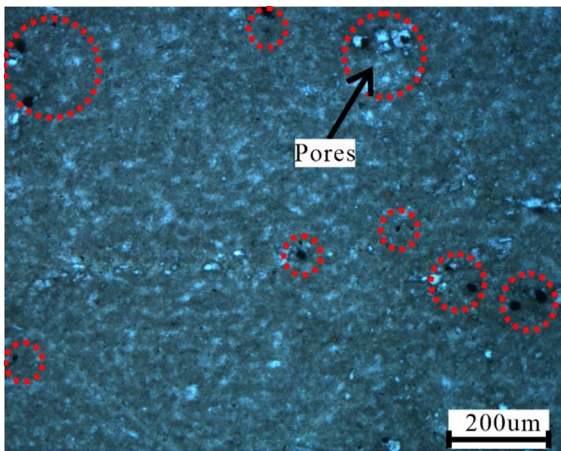


**Fig. 3** Microstructure of green mudstone (×50 times)

hydrophilic expansive mineral contributing to the expansive behavior of green mudstone. According to the literature, green mudstone is categorized as a microexpansive rock (Yan et al. 2004).

### 2.3 Test apparatus

As shown in Fig. 4, the main loading machine comprises a support frame, a base, a water tank, hydraulic loading bars, a glass, and cushion blocks. The support frame fixes the base and water tank (capacity = 3 L). During the test, the rock specimen is placed in this water tank. The upper and lower hydraulic loading bars are installed at the geometric center positions above and below the water tank to exert a maximum force of 400 kN on the specimen vertically. Three hydraulic loading bars are installed at the geometric center position of the left, right, and back sides of water tank to load the specimen horizontally. A glass window is installed at the front of the water tank to conveniently observe the changes in the rock specimen during the test. The cushion block is made of 25-mm-thick transparent plexiglass and is placed between the surface of the specimen and the indenter of the loading bar to ensure that the surface of the specimen is evenly stressed. Chamfering is set around each cushions block at a perimeter of C3 (3 × 45°) to prevent the cushion block from squeezing and rubbing against each other during loading. The experimental equipment is shown in Fig. 5.

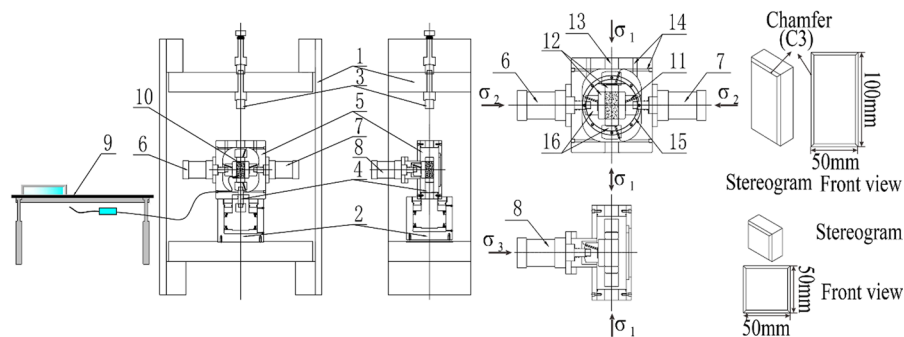
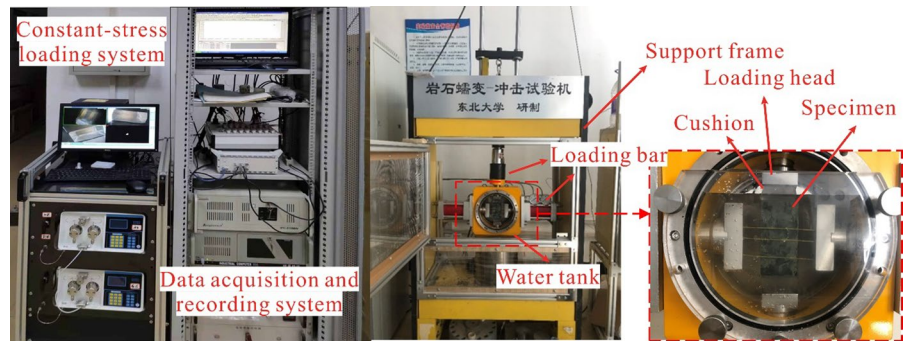


**Fig. 4** Immersion weakening experimental apparatus assembly drawing. 1, support frame; 2, base; 3, upper loading bar; 4, lower loading bar; 5, water tank; 6, left hydraulic loading bar; 7, right hydraulic loading bar; 8, rear hydraulic loading bar; 9,

information acquisition system; 10, specimen; 11, camera; 12, cushion block; 13, sealing hole of loading bar; 14, camera seal hole; 15, glass; 16, loading head

**Fig. 5** Immersion weakening experimental machine



### 3 Experimental results

#### 3.1 Results of water absorption test and uniaxial compressive strength test

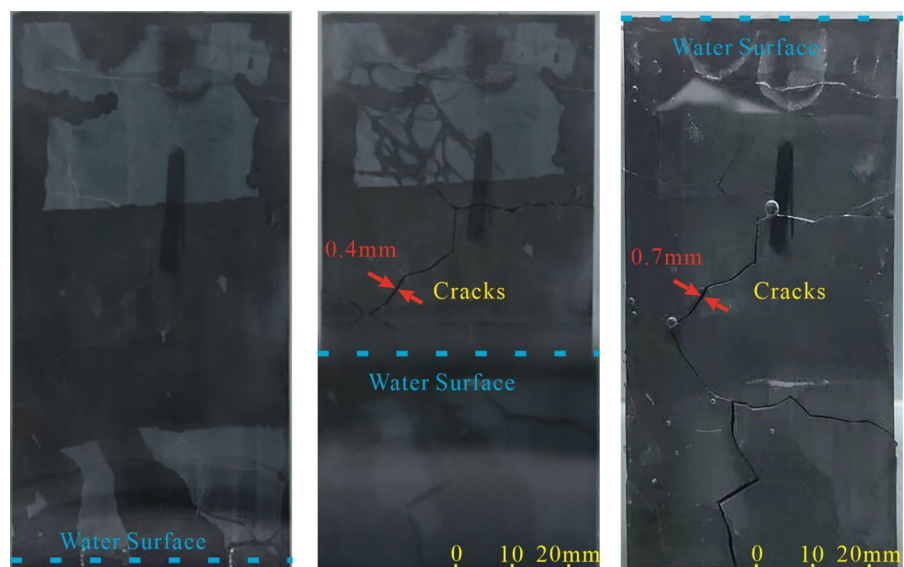
When the water level increased, water rapidly diffused into cracks (maximum crack opening was 0.4 mm) on the sample surface owing to capillary action, as shown in Fig. 6b. After submersion in water for 10 min, the specimens disintegrated, and the maximum crack opening was 0.7 mm, as shown in Fig. 6c.

The water content ( $w_t$ ) was measured every 5 min in the early stage and every hour in the late stage. Our findings showed that the water content of the rock specimen rapidly increased in the first 10 min (Fig. 7a), reaching 0.71%. After 4 h, no further changes were observed in the water content, and it

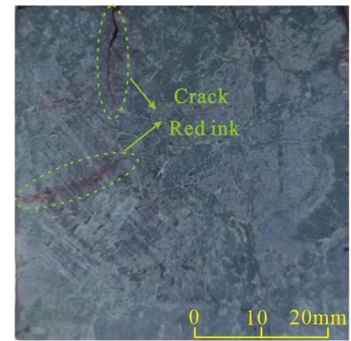
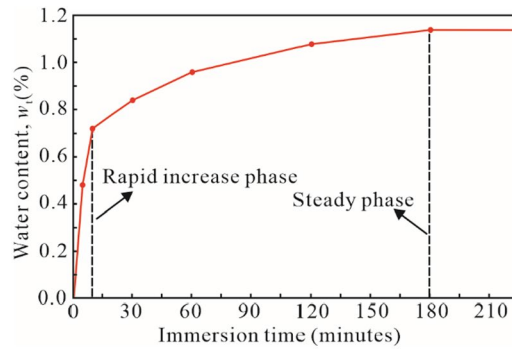
became stable at 1.15%. We soaked the specimen in red ink to observe the water distribution in the rock sample. After soaking for 4 h, the rock samples were removed and dried. Subsequently, the rock samples were transversely cut to observe their section. We found that the red ink mainly existed in large pores and cracks of the rock samples (Fig. 7b).

Table 1 shows the water content and UCS of specimens at different times. Figure 8a shows the relationship between immersion time and UCS, where the scatter points are the experimentally measured data and the red line is the fitted curve. The rate of decrease in UCS was greater during the first 10 min compared to other time. As the immersion time increased from 0 to 10 min and the peak strength decreased from 9.1 to 1.2 MPa, a decrease of 7.9 MPa was observed. However, when the immersion increased from 10 to 240 min, the peak strength decreased from 1.2 to

**Fig. 6** Failure of rock sample in water immersion without confining pressure



**Fig. 7** Water content of rock specimens at different times



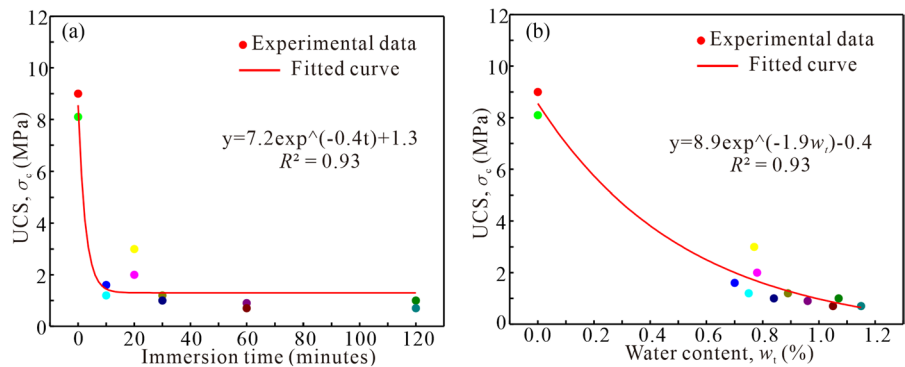
(a) Relationship between soaking time and water content

(b) Location of red link

**Table 1** Water content and uniaxial compressive strength (UCS) of specimens at different times

Immersion time (min)	0	10	20	30	60	120
Water content (%)	0	0.7	0.78	0.89	0.96	1.07
UCS(MPa)	9	1.6	2	1.2	0.9	1
	8.1	1.2	3	1	0.7	0.7

**Fig. 8** Relationship between immersion time (a), water content (b) and uniaxial compressive strength



0.7 MPa, which is a decrease of 0.5 MPa. Figure 8b shows the relationship between water content and UCS. A greater rate of decrease in UCS was observed at low water content than at high water content. As the water content increased from 0 to 0.71%, the peak strength decreased by 86.8%. The further increase in water content from 0.71 to 1.13% resulted in a 41.2% decrease in the peak strength. Figure 8 indicates the relationships between UCS and immersion time. UCS and water content can be best fitted using the following exponential equation:

$$f(x) = a \cdot e^{b \cdot x} + c \tag{4}$$

where  $f$  represents the UCS of green mudstone at immersion time or water content  $w_t$ , and  $a$ ,  $b$ , and  $c$  are constants. For the immersion time, the values of  $a$ ,  $b$ , and  $c$  were determined to be 7.2,  $-0.4$ , and 1.3, respectively. For  $w_t$ , the values were 8.9,  $-1.9$  and 0.4, respectively. These results are in good agreement with the findings of previous studies (Ergüler and Ulusay 2009; Masoumi et al. 2017).

The initial immersion time was unified at 10 min in a later immersion experiment under different confining pressure conditions because the water content and UCS of the rock changed after being soaked in water for 10 min.

### 3.2 Testing results of different immersion time

#### 3.2.1 Compressive strength analysis

The experimental data are shown in Table 2. The intermediate principal stress ( $\sigma_2$ ) plays an important role in the yield failure of rock (Drucker and Prager 1952). Figure 9a shows the relationship between  $\sigma_2$  and  $\sigma_1$  under dry and immersion conditions. The increasing rate of  $\sigma_1$  gradually decreased as  $\sigma_2$  increased. Under dry conditions, when  $\sigma_2$  increased from 0 to 0.5 MPa,  $\sigma_1$  increased from 9.1 to 15.1 MPa (i.e., an increase of 6 MPa). When  $\sigma_2$  further

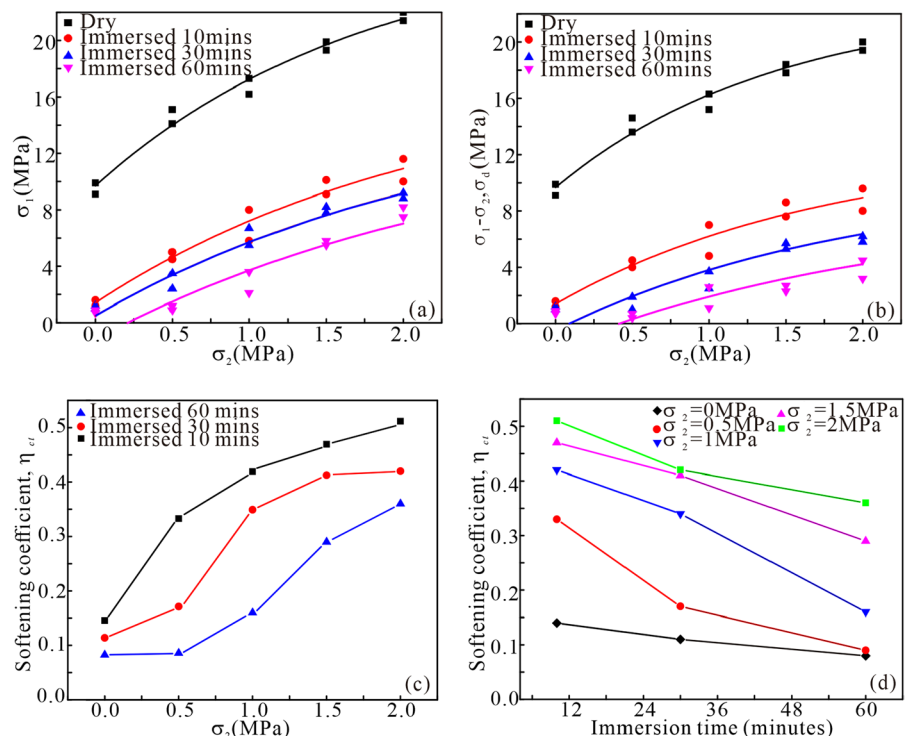
increased from 1.5 to 2 MPa,  $\sigma_1$  increased from 19.3 to 22 MPa (i.e., an increase of 2.7 MPa occurred). As shown in Fig. 9a, the increase in immersion time reduced the effect of  $\sigma_2$  on  $\sigma_1$ . When  $\sigma_2$  increased from 0 to 2 MPa,  $\sigma_1$  increased by 12.9 MPa in the dry state, 10.4 MPa in the soaked state for 10 min, and 6.9 MPa in the soaked state for 60 min.

The Fig. 9b shows the relationship between  $\sigma_2$  and  $\sigma_1 - \sigma_2$  under dry and immersion conditions. The failure criterion of mudstone is in good agreement with the exponential criterion (You 2009, 2011). The function expression is shown in Eq. (4), where  $c$  represents the limit of the difference between  $\sigma_1$

**Table 2** Maximum principal stress ( $\sigma_1$ ) under drying and immersion condition (unit: MPa)

$(\sigma_2, \sigma_3)$	(0.0,0.0)	(0.5,0.5)	(1.0,0.5)	(1.5,0.5)	(2.0,0.5)
Dry	9.9	15.1	17.3	19.3	22
	9.1	14.1	16.2	19.9	21.4
Immersed 10 min	1.6	5	5.8	9.1	10
	1.2	4.5	8	10.1	11.6
Immersed 30 min	1.2	3.5	5.5	7.8	9.2
	1	2.4	6.7	8.2	8.8
Immersed 60 min	0.9	1.2	2.1	5.5	8.2
	0.7	0.9	3.6	5.8	8.0

**Fig. 9** Analysis results of strength and softening coefficient. **a** Relationship between  $\sigma_2$  and  $\sigma_1$ ; **b** relationship between  $\sigma_2$  and  $\sigma_1 - \sigma_2$ ; **c** relationship between  $\sigma_2$  and softening coefficient; and **d** relationship between immersion time and softening coefficient





and  $\sigma_2(\sigma_d)$ . The value of  $c$  decreases with increasing immersion time.

The softening coefficient denotes the degree to which water weakens rock strength. The lower the softening coefficient, the greater the degree of weakening. Figure 9c shows that the softening coefficient of the specimen in each state increases with increasing  $\sigma_2$ . For specimens soaked in water for 10 min, the softening coefficient substantially reduced to 0.14 when  $\sigma_2$  was 0 MPa. However, the softening coefficient increased from 0.14 to 0.51 when  $\sigma_2$  increased from 0 to 2 MPa. For specimens soaked in water for 60 min, the softening coefficient increased from 0.08 to 0.36 when  $\sigma_2$  increased from 0 to 2 MPa.

Figure 9d shows that under the same confining pressure condition, the softening coefficient decreased as the immersion time increased. For specimens whose  $\sigma_2$  was 0 MPa, the softening coefficient was 0.14 when the soaking time was 10 min. However, the softening coefficient reduced to 0.08 when the soaking time was increased to 60 min. For specimens whose  $\sigma_2$  was 2 MPa, the softening coefficient reduced from 0.51 to 0.36 when the soaking time was increased from 10 to 60 min. If a weakening coefficient of less than 0.2 is considered as complete weakening, it can be achieved in 10 min when  $\sigma_2$  is 0 MPa, in 30 min when  $\sigma_2$  is 0.5 MPa, and in 60 min when  $\sigma_2$  is 1 MPa. Therefore, our findings show that the weakening effect of water on rock has a time effect; however, the increase in  $\sigma_2$  can delay the weakening time.

### 3.2.2 Failure mode analysis

The dry specimens experienced mainly vertical splitting failure was accompanied by a crisp sound, as shown in Fig. 10a and b, which present the front and side views of the specimens, respectively. As shown in Fig. 10b, the angle of the fracture plane is nearly vertical. Most broken parts of specimens are strips or sheets. When the rock specimens were loaded under water immersion conditions, the failure mode of the rock specimens was mostly shear failure. No distinct sound was noted during the failure, as shown in Fig. 10c and d, which present the front and side views of the specimens, respectively. As shown in Fig. 10c, the angle of the fracture plane is nearly horizontal or inclined at a certain angle and most of the broken bodies are lumps.

Figure 11 shows the failure process of the specimen soaked in water for 10 min; the different groups of cracks in the rock specimen are indicated by different colors. The crack opening in the middle of the rock specimens propagated first when the water level increased (Fig. 11b). The crack opening and internal elongation were considerably smaller than those in the water-immersed state with no confining pressure (Fig. 6). When  $\sigma_2$  was 0 MPa, the maximum opening was 0.7 mm and the maximum crack opening speed reached 0.36 mm/s. However, when  $\sigma_2$  was 2 MPa, the maximum opening was 0.23 mm and the maximum crack opening speed reached 0.06 mm/s.

After the specimen was soaked in water for 6 min, the transverse crack of the specimen surface began to

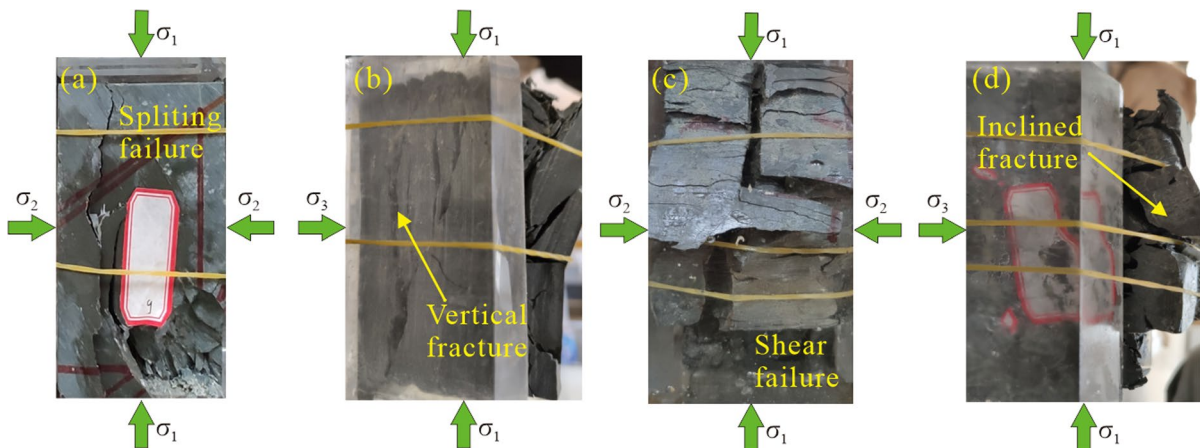
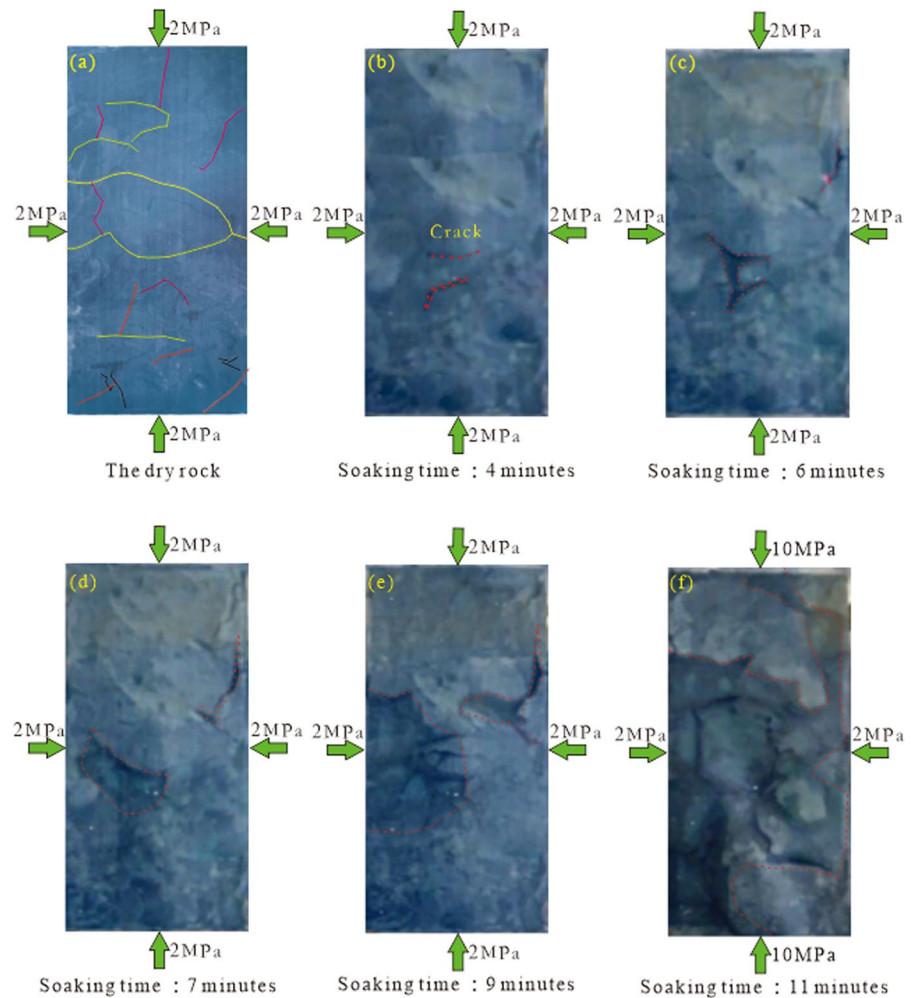


**Fig. 10** Failure modes of dried and immersed specimens. **a** and **b** are dried specimens; **c** and **d** are immersed specimen

**Fig. 11** Failure process of specimens in water immersion after compression



penetrate up and down, accompanied by flake peeling. Simultaneously, the vertical crack in the upper right part extended (Fig. 11c). Further peeling of the specimen surface caused complete penetration of the upper and lower cracks in the middle of the rock specimen, resulting in the formation of a small wedge-shaped pit. The vertical cracks in the upper right part continued to expand, as shown in Fig. 11d.

The presence of the wedge-shaped pit reduced the restriction of the rock specimen near the side of the pit. Because of the continuous softening of new cracks and the interior of the rock due to water, large fragments of the specimens began to fall and the range and depth of the wedge-shaped pit expanded (Fig. 11e). The combined action of water and load caused the upper vertical cracks and wedge-shaped

pits to continuously expand, and the rock specimen eventually failed, as illustrated in Fig. 11f.

### 3.2.3 Shear strength analysis

In 1952, Drucker and Prager (1952) proposed the generalized Mises yield and failure criterion considering the effect of hydrostatic pressure, as shown in Eq. (5). When  $f=0$ ,  $\sqrt{J_2}$  has a linear relationship with  $I_1$ , while  $\alpha$  and  $K$  are experimental constants related to friction angle  $\varphi$  and cohesion  $c$ , respectively. In the analysis,  $\sqrt{J_2}$  and  $I_1$  are obtained by calculating the experimental data. Thereafter,  $\alpha$  and  $K$  are obtained by linear fitting, where the cohesion and friction angles are further calculated (Colmenares and Zoback 2002; Yi et al. 2005, 2006).

$$f = \alpha I_1 + \sqrt{J_2} - K = 0 \tag{5}$$

$$I_1 = \sigma_1 + \sigma_2 + \sigma_3, J_2 = \frac{1}{6} [(\sigma_1 - \sigma_3)^2 + (\sigma_2 - \sigma_3)^2 + (\sigma_3 - \sigma_1)^2] \tag{6}$$

In the  $\pi$  plane, if the D-P criterion is the circumcircle of a Coulomb hexagon, then:

$$\alpha = \frac{2 \sin \varphi}{\sqrt{3}(3 - \sin \varphi)}, K = \frac{6c \cos \varphi}{\sqrt{3}(3 - \sin \varphi)} \tag{7}$$

The cohesion and friction angle under different immersion times can be obtained using Eqs. (5)–(7), as shown in Fig. 12. The rate of decrease in friction angle and cohesion was greater during the first 10 min than at other times. The friction angle and cohesion of the dry specimens were 47.8° and 2.27 MPa. When the immersion time was 10 min, the friction angle and cohesion became 45.5° and 0.56 MPa, a decrease of 2.3° and 1.71 MPa, respectively. When the immersion time was increased from 10 to 60 min, the friction angle and cohesion were 41.7° and 0.06 MPa, a decrease of 3.8° and 0.5 MPa, respectively.

The cohesion of rock is determined by the degree of cementation between mineral particles, and the friction angle is determined by the roughness between mineral particles. Under water soaking, water mainly reduces the cementation strength between minerals and has little influence on the roughness of minerals (Yu et al. 2015; Fu et al. 2019). Moreover, the previous chapters have shown that the mudstone of the Fushun West Open-pit is significantly weakened by

water, especially in the absence of confining pressure. Compared with the dried specimen, the cohesion and friction angle of mudstone decreased by 75% and 5%, respectively, after 10 min of immersion. Thus, the effect of water on cohesion is much greater than that of friction angle.

### 3.3 Analysis of creep results

#### 3.3.1 Evolution of creep strain

The specimens failed after being subjected to 2 to 5 stress levels. The stress increment at each level was 4 MPa and the loading time was 10 h. The longest time was 43.5 h. Figure 13 shows the stress–time and strain–time curves of the dried, saturated, and soaking specimen. The test results are shown in Table 3.  $\epsilon_0$ ,  $\epsilon_c$ , and  $\epsilon_t$  are the initial strain ( $\times 10^{-2}$ ), creep strain ( $\times 10^{-2}$ ), and total strain ( $\times 10^{-2}$ ), respectively.  $t_f$  is the time to failure at the final stress level.

The dried specimen experienced five stress levels, and the total failure time was 43.5 h. The instantaneous strain was  $0.84 \times 10^{-2}$  when the stress level was 4 MPa. The strain increased as the strain rate decreased when the creep entered the deceleration phase. The initial strain increased to  $1.31 \times 10^{-2}$  when the stress level was 8 MPa. A further increase in stress level to 20 MPa resulted in the strain reaching the long-term strength of the specimen. After experiencing the deceleration phase, the strain entered the accelerating phase, which led to the failure of the specimen.

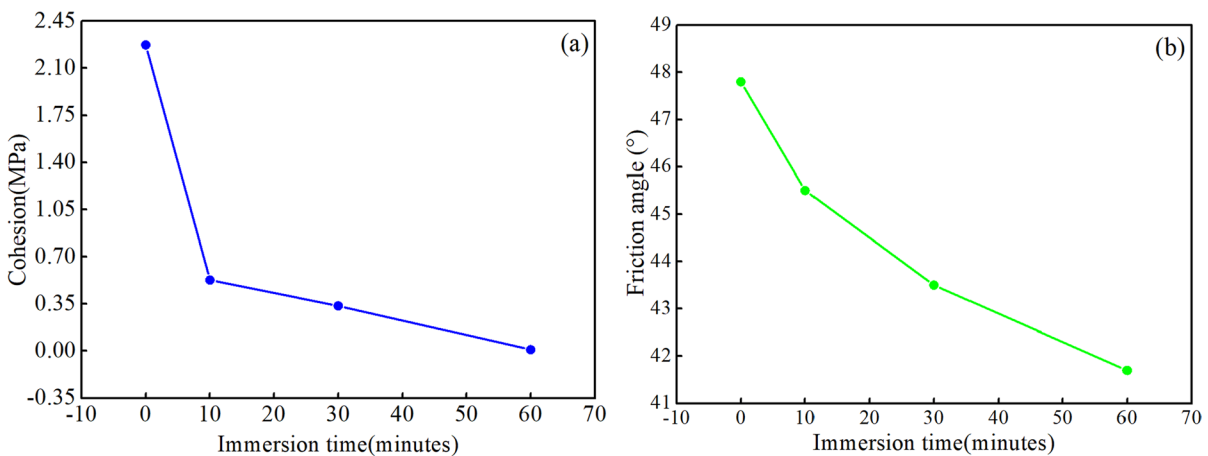
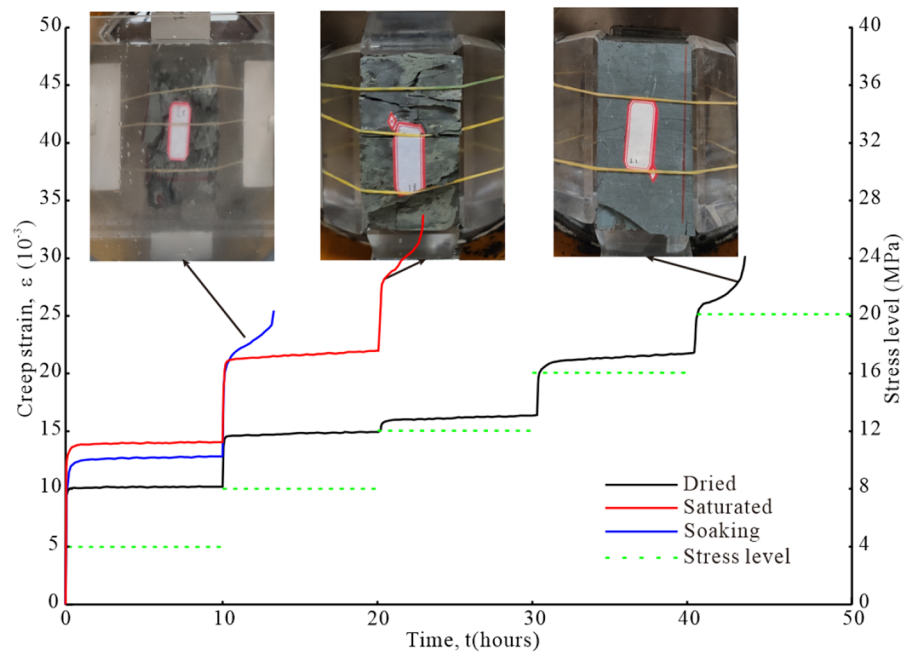
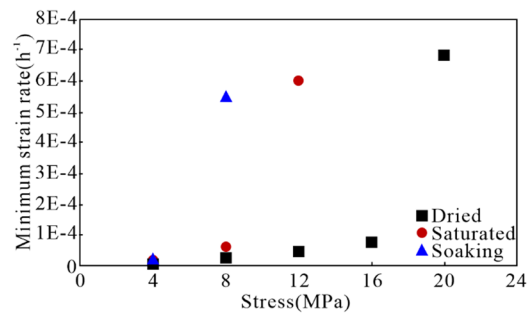


**Fig. 12** Cohesion (a) and friction angle (b) under different immersion time

**Fig. 13** Creep test result of the dried, saturated and soaking specimens



(a) Creep strain of the dried, saturated, and soaking specimens



(b) Minimum strain rate of the dried, saturated and soaking specimens

**Table 3** Creep parameters of specimens at different stress levels

Specimen	4 MPa			8 MPa			12 MPa			16 MPa			20 MPa			
	$\epsilon_0$	$\epsilon_c$	$\epsilon_t$	$\epsilon_0$	$\epsilon_c$	$\epsilon_t$	$\epsilon_0$	$\epsilon_c$	$\epsilon_t$	$\epsilon_0$	$\epsilon_c$	$\epsilon_t$	$\epsilon_0$	$\epsilon_c$	$\epsilon_t$	$t_f$
Dried	0.84	0.12	0.96	1.31	0.12	1.43	1.45	0.13	1.58	1.85	0.27	2.12	2.24	0.78	3.02	3.5
Saturated	1.19	0.22	1.41	1.88	0.3	2.18	2.61	0.75	3.37							2.8
Soaking	0.95	0.33	1.28	1.81	0.72	2.53										3

The initial strain of the saturated specimen was larger than that of the dry specimen, owing to the damage caused by water; it was  $1.19 \times 10^{-2}$ , i.e., 1.4 times that of the dry specimen, when the stress level was 4 MPa. The strain stabilized to a constant value

after 3 h. When the stress level was 12 MPa, the specimen failed completely.

Water weakening had a time effect and was influenced by confining pressure, as discussed in the previous chapter. In the creep test of the



soaking specimen, when the stress increased to 4 MPa, the water did not react with the rock. As a result, the initial strain of the soaking specimen was slightly larger than that of the dried specimen, which was  $0.95 \times 10^{-2}$ . With increasing soaking time, the strain rate had multiple increase–decrease phases. The constant reaction between water and rock made the strain rate at the deceleration phase greater than that of the saturated specimen. After soaking in water for 10 h, the stress level was 8 MPa and the initial strain was  $1.81 \times 10^{-2}$ . Under axial loading, the rock developed many microcracks, which intensified the weakening of the rock by water and reduced the long-term strength of the rock to less than that of the saturated specimen.

Figure 13b shows that the strain rate during creep increased due to increasing applied stress; the creep rate increased suddenly at the failure stress level (Heap et al. 2009, 2015). Additionally, the strain rate of the soaking specimens is the maximum while that of the dried specimens is the minimum. With increasing soaking time, the rock constantly reacts with water, rapidly increasing the strain rate. When the stress level was 4 MPa, the strain rate of the soaking specimen was 7.5 times that of the dried specimen and 1.1 times that of the saturated specimen. However, in the next stress level, the strain rate of the soaking specimen was 22 times that of the dried specimen and 9 times that of the saturated specimen.

### 3.3.2 Analysis of the initial creep

Figure 14a shows the relationship between the initial strain and stress. The saturated and soaking specimens represented two types of water-containing states of the specimen. Therefore, the creep characteristics of soaked and saturated specimens were compared. In the first stress loading level, the initial strain of the soaking and dried specimens was similar; however, the initial strain of the soaking specimen was smaller than that of the saturated specimen: the difference was  $0.24 \times 10^{-2}$ . When the stress level increased from 4 to 8 MPa, the initial strain of the soaking specimen increased by 0.86 while that of the dried and saturated specimens increased by 0.47 and 0.69, respectively. As the soaking time increased, the rock approached saturation. Therefore, when the stress was 8 MPa, the initial strain of the soaking specimen differed from that of the saturated specimen by  $0.07 \times 10^{-2}$ .

Figure 14b shows the relationship between total strain and stress. When the stress level was set to 4 MPa, the total strain of the soaking specimen was smaller than that of the saturated specimen; the difference between the specimens was  $0.13 \times 10^{-2}$ . When the stress level was 8 MPa, the total strain of the soaking specimen was greater than that of the saturated specimen; the difference between the specimens was  $0.35 \times 10^{-2}$ .

Figure 14 shows that the creep curve of the soaking specimen in the initial state is the same as that of

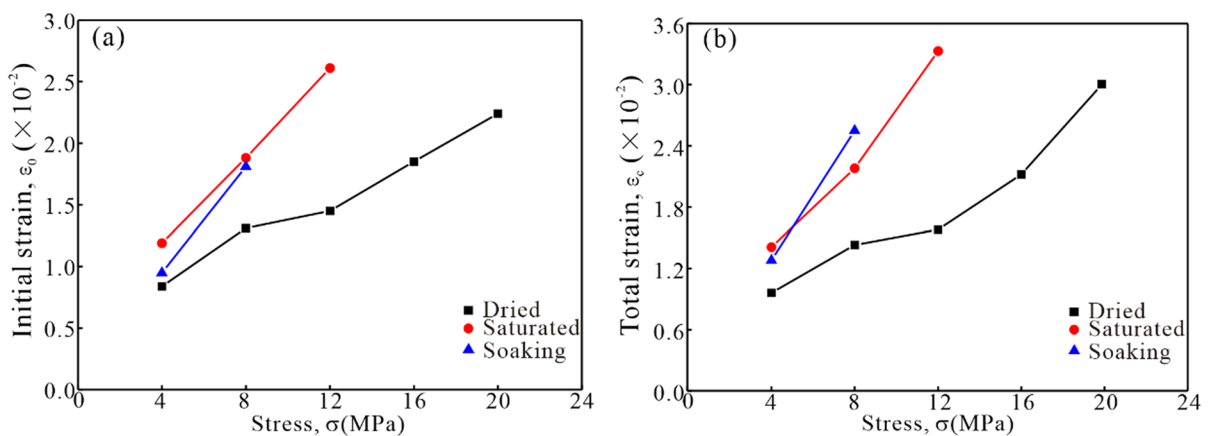


**Fig. 14** The instantaneous strain (a) and total strain (b) at different stress level

the dried specimen. With increasing soaking time, the water content of the soaking specimens increased continuously. Under the softening effect of water, the rock strength gradually decreased and the rock creep behavior gradually approached the saturated specimen. In the creep test, the rock is prone to produce new cracks under the action of water. An increase in fractures increases the water content of mudstone. With increasing immersion time, water continuously softens the fractures and erodes the interior of rocks through the fractures, further reducing the overall strength of mudstone. Therefore, the deformation characteristics of soaking specimens become increasingly obvious and gradually exceed that of saturated specimens.

### 3.3.3 Critical stress level for creep failure

Figure 15 shows the relationship between  $\omega$  and stress level. The increase or decrease in  $\omega$  indicates the increase or decrease in the creep behavior, respectively. For the dried specimen,  $\omega$  gradually decreased with increasing stress, indicating that the creep behavior decreased when stress was between 0 and 12 MPa. When stress was > 12 MPa,  $\omega$  began to increase, indicating that the creep behavior began to increase. When stress was > 16 MPa,  $\omega$  increased sharply and the corresponding creep behavior accelerated. Therefore, the critical stress of dried specimens was 12–16 MPa, accounting for 54–73% of the peak strength. Similarly, in the case of saturated specimens,  $\omega$  gradually decreased when the stress

level was < 8 MPa. However, when the stress level was > 8 MPa,  $\omega$  gradually increased; therefore, the critical stress of the saturated specimen was 8 MPa. The soaking specimen had only 2 stress phases and no descent phase. In the case of the soaking specimen,  $\omega$  gradually increased when the stress level exceeded 4 MPa. Therefore, the critical stress of the soaking specimen was 4 MPa.

## 4 Discussion

In this study, we examined the effects of confining pressure and soaking time on rock strength using the experimental loading and soaking methods simultaneously; this approach differs from those discussed in the literature (Ulusay et al. 2015; Vergara et al. 2016; Zhou et al. 2016). Based on previous studies on the weakening effect of water on rocks, researchers have generally soaked the specimens in water first and then conducted mechanical loading after achieving the set water content state (Baud et al. 2000; Dan et al. 2012). These tests can maximize the weakening effect of water on rocks but does not consider the timeliness of water erosion. Our research findings confirmed that confining pressure and time affect the weakening effect of water on rocks. When the confining pressure is substantially low, the weakening coefficient of rock becomes large in a considerably short time (10 min). Notably, the increase in confining pressure inhibits the weakening effect and prolongs the weakening time. Therefore, analyzing the results of the uniaxial water soaking test will overestimate the weakening effect of actual reclaimed water on rock slopes.

Our findings also showed that water mainly exists in cracks and pores of rocks. Therefore, we manually measured the crack openings and compared the crack growth results under different confining pressures. We found that the maximum crack aperture reached 0.7 mm and the crack aperture velocity reached 0.36 mm/min when  $\sigma_2$  was 0 MPa. However, the maximum crack aperture reached 0.23 mm and the crack aperture velocity reached 0.06 mm/min when  $\sigma_2$  was 2 MPa (Fig. 16). Therefore, the confining pressure limits the crack aperture, affecting the speed of water entering the rock. Our analysis of the effect of immersion time on the friction angle and cohesion of mudstone showed that the weakening effect of water

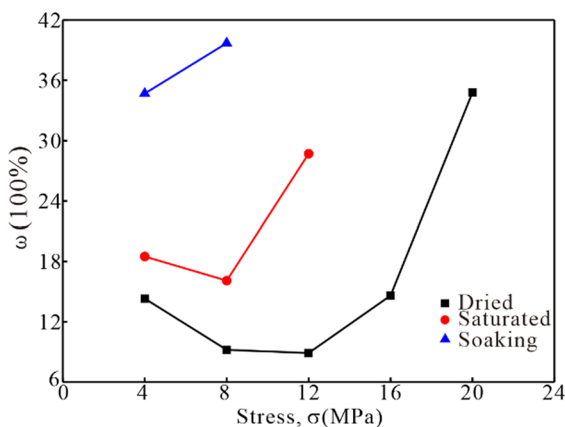


**Fig. 15** Relationship between creep strain rate ( $\omega$ ) and stress

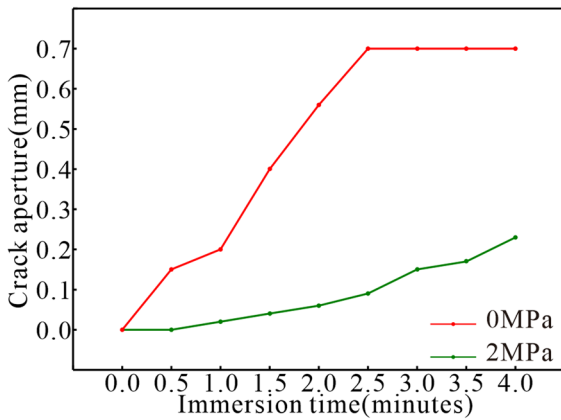


**Fig. 16** Crack aperture under different soaking times

on the cohesion was stronger than that on the friction angle. This finding agrees with those reported by other researchers (Fu et al. 2019; Liu et al. 2020).

Among the three water-bearing states in the creep experiment in this study, the research results of soaking specimens are rarely studied. In actual water-filled slopes, water continuously erodes the rock mass (Nakamura 1990). Compared with the saturated specimen, soaking specimens can improve the reflection of the creep behavior of rock under long-term immersion in water. In the long-term deformation process of soaking specimens, water continuously enters the rock through cracked microfissures, accelerating rock deformation and causing failure earlier than that of saturated specimens. Accordingly, the stress phase in the case of soaking specimens was minimum.

Our research results also showed that the fracture-developed area and low confining pressure area were the most seriously eroded areas during the process of water filling. Therefore, conducting detailed geological surveys before impounding the Fushun West Open pit is necessary. The slope of the Fushun West Open pit mine formed an unloading fracture zone at a maximum depth of 66 m from the surface of the slope owing to excavation disturbance and weathering disturbance. The fractures in this zone are developed, and the quality of rock mass is poor. Therefore, backfill treatment should be performed in these areas before water storage, as shown in Fig. 17. Backfill dumping is a natural antiseepage material and plays a role in stabilizing the slope. Compared with dried mudstone, the stress threshold and failure time of creep failure of soaking mudstone are reduced by 4

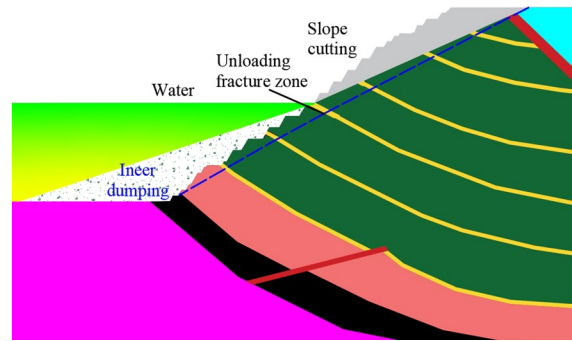


**Fig. 17** Cross-section of water storage treatment in Fushun West Open pit

times and 3 times, respectively. Therefore, stress monitoring is essential in the process of water storage.

### 5 Conclusion

In this study, we examined the weakening regularity of green mudstone at different confining pressures and immersion times using self-developed apparatus to analyze the impact of water storage on mudstone after the closure of the Fushun West Open pit. For the creep test, mudstone was immersed in water under a confining pressure of 2 MPa and was compared with dry and saturated specimens. The main findings of our study are as follows:

- (1) The existence of cracks substantially reduced the UCS of mudstone in a short time. The UCS decreased exponentially with increasing water content. After soaking for 10 min, the UCS decreased to 14% of that of the dried specimen.
- (2) The failure criterion of mudstone under different confining pressures conformed to the exponential strength criterion. The increase in confining pressure limited the expansion of the crack aperture, reducing the speed and content of the water entering the rock, which ultimately reduced the water-weakening coefficient and delayed the weakening time. The weakening coefficient with confining pressure was 3.4–4.5 times that without confining pressure. If the same degree of weakening was obtained, it took only 10 min to immerse in water without confining pressure and 60 min

to immerse in water with a confining pressure of 1.5 MPa.

- (3) Water can alter the failure mode of mudstone. The splitting failure of dry mudstone and the shear failure of soaking mudstone simultaneously occurred during loading. The cohesion and friction angle of mudstone decreased rapidly during the initial soaking phase and tended to stabilize with increasing soaking time. During the soaking process, water considerably weakened cohesion more than the friction angle.
- (4) The creep behavior of mudstone changed significantly with the change in the water condition. The soaking specimen had the lowest stress level for creep failure and the shortest failure time for the three types of test specimens. The creep curve of the soaking specimen was the same as that of the dry specimen during the initial phase. However, as soaking time increased, the weakening effect of water on the specimen increased, causing the creep curve of the soaking specimen to approach that of the saturated specimen. Water entered the microcrack and reacted with the rock interior, causing the rock to fail rapidly.
- (5) The ratio of creep strain to initial strain decreased first and then increased, and the stress level at the inflection point was considered the critical stress of creep failure. The critical stress of the soaking sample was lower than that of the saturated and dry specimens.

**Acknowledgements** This work was supported by the National Key Research and Development Program of China (2022YFC2903902) and (2022YFC2903903) and the National Science Foundation of China (U1903216).

#### Declarations

**Conflict of interest** The author(s) declared no potential conflict of interest with respect to the research, authorship, and/or publication of this article.

**Open Access** This article is licensed under a Creative Commons Attribution 4.0 International License, which permits use, sharing, adaptation, distribution and reproduction in any medium or format, as long as you give appropriate credit to the original author(s) and the source, provide a link to the Creative Commons licence, and indicate if changes were made. The images or other third party material in this article are included in the article's Creative Commons licence, unless indicated otherwise in a credit line to the material. If material is not included in the article's Creative Commons licence and your

intended use is not permitted by statutory regulation or exceeds the permitted use, you will need to obtain permission directly from the copyright holder. To view a copy of this licence, visit <http://creativecommons.org/licenses/by/4.0/>.

#### References

- ASTM (2005) D2216–10 standard test methods for laboratory determination of water (moisture) content of soil and rock by mass. ASTM International, United States
- Baud P, Zhu W, Wong TF (2000) Failure mode and weakening effect of water on sandstone. *J Geophys Res Sol Ea* 105(B7):16371–16389
- Brady NC, Weil RR (1960) The nature and properties of soils. The nature and properties of soils: Macmillan Company
- Brantut N, Heap MJ, Meredith PG, Baud P (2013) Time-dependent cracking and brittle creep in crustal rocks: a review. *J Struct Geol* 52:17–43
- Bonnelye A, Schubnel A, David C, Henry P, Guglielmi Y, Gout C, Dick P (2017) Strength anisotropy of shales deformed under uppermost crustal conditions. *J Geophys Res Sol Ea* 122(1):110–129
- Chen KT, Wu JH (2018) Simulating the failure process of the Xinmo landslide using discontinuous deformation analysis. *Eng Geol* 239:269–281
- Colmenares LB, Zoback MD (2002) A statistical evaluation of intact rock failure criteria constrained by polyaxial test data for five different rocks. *Int J Rock Mech Min Sci* 39(6):695–729
- Dan Z, Anqiang C, Gangcai L (2012) Laboratory investigation of disintegration characteristics of purple mudstone under different hydrothermal conditions. *J Mt Sci* 9(001):127–136
- Drucker DC, Prager W (1952) Soil mechanics and plastic analysis or limit design. *Q Appl Math* 10:157–165
- Ergüder ZA, Ulusay A (2009) Water-induced variations in mechanical properties of clay-bearing rocks. *Int J Rock Mech Min* 46:355–370
- Farulla CA, Ferrari A, Romero E (2010) Volume change behaviour of a compacted scaly clay during cyclic suction changes. *Can Geotech J* 47(6):688–703
- Fu H, Liu J, Zeng L, Bian H, Shi Z (2019) Deformation test of pre-disintegrating carbonaceous mudstone under loading and foundering condition. *Rock Soil Mech* 40(04):1273–1280 ((In Chinese))
- Gutierrez F, Lucha P, Galve JP (2010) Reconstructing the geochronological evolution of large landslides by means of the trenching technique in the yesa reservoir. *Geomorphology* 124(3–4):124–136
- Geng Z, Bonnelye A, Chen M, Jin Y, Dick P, David C, Schubnel A (2017) Elastic anisotropy reversal during brittle creep in shale. *Geophys Res Lett* 44(21):10–887
- Geng Z, Bonnelye A, Chen M, Jin Y, Dick P, David C, Schubnel A (2018) Time and temperature dependent creep in Tournemire shale. *J Geophys Res Sol Ea* 123(11):9658–9675
- He L, Wu L, Liu S (2015) Mapping two-dimensional deformation field time-series of large slope by



- coupling DInSAR-SBAS with MAI-SBAS. *Remote Sens* 7(9):12440–12458
- Heap MJ, Baud P, Meredith PG, Bell AF, Main IG (2009) Time-dependent brittle creep in Darley Dale sandstone. *J Geophys Res Solid Earth* 114
- Heap MJ, Brantut N, Baud P, Meredith PG (2015) Time-dependent compaction band formation in sandstone. *J Geophys Res Solid Earth* 120:4808–4830
- Huang H, Che P (2007) Research on micro-mechanism of softening and argillitization of mudstone. *J Tongji Univ* 35(7):866 ((In Chinese))
- Huang D, Gu DM, Song YX, Cen DF, Zeng B (2018) Towards a complete understanding of the triggering mechanism of a large reactivated landslide in the three gorges reservoir. *Eng Geol* 238:36–51
- Israelachvili JN, Mcguiggan PM (1988) Forces between surfaces in liquids. *Science* 16(1):31–47
- ISRM (2007) The complete ISRM suggested methods for rock characterization, testing and monitoring: 1974–2006. In: Ulusay R, E HJ (eds) Suggested methods prepared by the commission on testing methods, international society for rock mechanics. Compilation arranged by the ISRM Turkish National Group, Ankara, Turkey
- Jiao YY, Zhang HQ, Tang HM, Zhang XL, Adoko AC, Tian HN (2014) Simulating the process of reservoir-impoundment-induced landslide using the extended DDA method. *Eng Geol* 182:37–48
- Jones FO, Embody DR, Peterson WL, Hazlewood RM (1961) Landslides along the columbia river valley, northeastern washington, with a section on seismic surveys
- Johnson EA (1990) Geology of the Fushun coalfield, Liaoning province, people's republic of China. *Int J Coal Geol* 14(3):217–236
- Li D, Wang W (2019) Quantitative analysis of the influence of saturation on rock strength reduction considering the distribution of water. *Geomech Geophys Geo* 5:197–207
- Liu X, Tang Z, Li LU, Zhang Q, Su F (2020) Experimental study on shear properties of red sandstone joints after cyclic wetting-drying treatment. *Chin J Rock Mech Eng* 39(S2):3316–3325 ((In Chinese))
- Liu S, Wang H, Huang J (2015) High-resolution remote sensing image-based extensive deformation-induced landslide displacement field monitoring method. *Int J Coal Sci Technol* 2(3):170–177
- Macfarlane DF (2009) Observations and predictions of the behavior of large, slow moving landslides in schist, Clyde dam reservoir. *N Z Eng Geol* 109(1):5–15
- Masoumi H, Horne J, Timms W (2017) Establishing empirical relationships for the effects of water content on the mechanical behavior of gosford sandstone. *Rock Mech Rock Eng* 50:1–8
- Ma L (2004) Experimental investigation of time dependent behavior of welded Topopah Spring tuff. University of Nevada. In: Reno
- Mikroutsikos A, Theocharis AI, Koukoulas NC, Zevgolis IE (2021). Slope stability of deep surface coal mines in the presence of a weak zone. *Geomech Geophys Geo* 7(3)
- Nakamura K (1990) On reservoir landslide. *B Soil Water Conserv* 10(1):53–64 ((In Chinese))
- Rybacki E, Reinicke A, Meier T, Makasi M, Dresen G (2015) What controls the mechanical properties of shale rocks-part I: strength and Young's modulus. *J Petrol Sci Eng* 135:702–722
- Rybacki E, Meier T, Dresen G (2016) What controls the mechanical properties of shale rocks-Part II: brittleness. *J Petrol Sci Eng* 144:39–58
- Rybacki E, Herrmann J, Wirth R, Dresen G (2017) Creep of Posidonia shale at elevated pressure and temperature. *Rock Mech Rock Eng* 50(12):3121–3140
- Sun SW, Liu L, Hu JB, Ding H (2022) Failure characteristics and mechanism of a rain-triggered landslide in the northern longwall of fushun west open pit, china. *Landslides* 19(10):2439–2458
- Tang S (2018) The effects of water on the strength of black sandstone in a brittle regime. *Eng Geol* 239:167–178
- Tarifard A, Görög P, Török Á (2022) Long-term assessment of creep and water effects on tunnel lining loads in weak rocks using displacement-based direct back analysis: an example from northwest of Iran. *Geomech Geophys Geo* 8(1):31
- Tu G, Huang D, Huang R, Deng H (2019) Effect of locally accumulated crushed stone soil on the infiltration of intense rainfall: a case study on the reactivation of an old deep landslide deposit. *B Eng Geol Environ* 78:4833–4849
- Ulusay R, Karakul H (2015) Assessment of basic friction angles of various rock types from turkey under dry, wet and submerged conditions and some considerations on tilt testing. *B Eng Geol Environ* 28(4):1–17
- Vergara MR, Triantafyllidis T (2016) Influence of water content on the mechanical properties of an argillaceous swelling rock. *Rock Mech Rock Eng* 49(7):2555–2568
- Wang R, Nie L (2010) Landslide prediction in Fushun west open pit mine area with quadratic curve exponential smoothing method. In: 2010 18th international conference on geoinformatics IEEE
- Xue Y, Xu T, Heap MJ, Meredith PG, Mitchell TM, Wasantha PLP (2023) Time-dependent cracking and brittle creep in macrofractured sandstone. *Int J Rock Mech Min Sci* 162:105305
- Xue Y, Xu T, Zhu W, Heap MJ, Heng Z, Wang X (2021) Full-field quantification of time-dependent and-independent deformation and fracturing of double-notch flawed rock using digital image correlation. *Geomech Geophys Geo* 7(4):1–15
- Yan SX, Qu YX, Han SJ (2004) A study on the relationship between smectite content and swell potential indices. *J Eng Geol* 01:74–82 ((In Chinese))
- Yang T, Xu T, Liu H, Zhang C, Wang S, Rui Y (2014) Rheological characteristics of weak rock mass and effects on the long-term stability of slopes. *Rock Mech Rock Eng* 47(6):2253–2263
- Yi X, Valkó PP, Russell JE (2005) Effect of rock strength criterion on the predicted onset of sand production. *Int J Geomech* 5(1):66–73
- Yi X, Ong S, Russell JE (2006) Quantifying the effect of rock strength criteria on minimum drilling mud weight prediction using poly axial rock strength test data. *Int J Geomech* 6(4):260–268
- You M (2009) True-triaxial strength criteria for rock. *Int J Rock Mech Min* 46:115–127

- You M (2011) Strength and damage of marble in ductile failure. *J Rock Mech Geotech* 3:161–166
- Yu C, Tang S, Tang C, Duan D, Zhang Y, Liang Z (2019) The effect of water on the creep behavior of red sandstone. *Eng Geol* 253:64–74
- Yu J, Chen X, Li H, Zhou JW, Cai YY (2015) Effect of freeze-thaw cycles on mechanical properties and permeability of red sandstone under triaxial compression. *J Mt Sci* 12(1):218–231
- Yuan Y, Xu T, Heap MJ (2021) A three-dimensional mesoscale model for progressive time-dependent deformation and fracturing of brittle rock with application to slope stability. *Comput Geotech* 135:104160
- Zhang F, Yang T, Li L, Wang Z, Xiao P (2019) Cooperative monitoring and numerical investigation on the stability of the south slope of the fushun west open-pit mine. *B Eng Geol Environ* 78(4):2409–2429
- Zhang F, Yang T, Li L (2021) Assessment of the rock slope stability of fushun west open-pit mine. *Arab J Geosci* 14(15):1–20
- Zhou Z, Cai X, Cao W, Li X, Xiong C (2016) Influence of water content on mechanical properties of rock in both saturation and drying processes. *Rock Mech Rock Eng* 49(8):3009–3025

**Publisher's Note** Springer Nature remains neutral with regard to jurisdictional claims in published maps and institutional affiliations.